World Applied Sciences Journal 26 (11): 1428-1433, 2013
ISSN 1818-4952

DOI: 10.5829/idosi.wasj.2013.26.11.13582

Microstructure and Current-Voltage Characteristics of Vanadium-Doped Zinc Oxide-Based Varistors

[1]Saber E. Mansour, [1]Osama A. Desouky, [2]El-Sayed M. Negim, [3]G. Irmukhametova and [3]R.A. Mangazbayeva

[1]Department of Chemistry, Faculty of Science,
Omar Al-Mukhtar University, Box 919, Al-Bayda, Libya
[2]Faculty of Science and Engineering, University of Wolverhampton,
Wulfruna Street Wolverhampton, West Midlands, WV1 1LY, UK
[3]Department of Organic Substances, Chemistry and Technology, Natural Compounds and Polymers,
Al-Faraby Kazakh National University, 050038 Almaty, Kazakhstan

Submitted: Oct 29, 2013; **Accepted:** Nov 28, 2013; **Published:** Dec 2, 2013

Abstract: The present study deals with microstructure, electrical properties, water absorption and firing shrinkage of V_2O_5 doped ZnO in the range of 0.1 - 1mol% V_2O_5, which fired at temperatures range of 800-1220 ^{0} C for different soaking times. Densification of the suggested mixes is deduced from physical properties of water absorption and firing shrinkage. A decrease in water absorption was recorded with rise in maturing temperature and increase in time of soaking but the results of firing shrinkage showed an increase with rise in temperature and soaking time. The samples are examined by using X-ray diffraction patterns (XRD), scanning electron microscope (SEM) and DC electrical measurements. XRD data indicate that no secondary phases are formed, supporting the SEM results.

Key words: Microstructure · Electrical properties · Firing shrinkage · X-Ray diffraction · Varistor

INTRODUCTION

Ceramics based on zinc oxide doped with metal oxides are the common materials for varistors. High temperature firing is the most important stage in their manufacturing. This produces the phases and the granular structure required which give rise at the grain boundaries to potential Marries that are responsible for the nonlinear electrical behavior. During firing densification takes place and the density of the fired compact could reach the solid density depending on several parameters, one of which is the metal oxide additives can be one or several of oxides of Bi, Co Mn, Sb, Ti or Li. Trontelj and Kojar [1] studied the sintering of ZnO-based ceramics. They found that the addition of 0.5% Li_2O to ZnO shifts the onset of sintering towards 600°C, where the shrinkage starts; and the addition of Sb_2O_3 to ZnO shifts the onset of sintering to higher temperatures (1000°C). This was also observed by Marshall *et al*. [2]. Chu *et al*, [3] studied the effect of heating rate on the densification of ZnO to powder compacts using samples with the same initial relative density (50%). The heating rates used were 0.5, 2.5,10 and 15°C/min. They carried out the tests using a dilatometer by heating the sample to 500°C at 160C/min then using one of the above heating rates up to 1000°C. They found that the higher the heating rate the higher the temperature at which densification starts. They also noted that the final densities obtained independent of the heating rate. Huckabee and Palmour III [4] studied the rate controlled sintering of $A1_2O_3$ containing 0.1% MgO. They reported that the conventional standard firing curves does not represent an optimum for $A1_2O_3$ because its earlier densification rates are excessive which create trapped pores. Non-ohmic behavior of zinc oxide ceramics is achieved by merely doping with either Bi_2O_3, or BaO [5-9].

Corresponding Author: Saber E. Mansour, Omar Al-Mukhtar University, Department of Chemistry, Al-Bayda, Libya.
Tel: +218 91 376 7134.

These dopants will segregate at the grain boundary during sintering and form an electronic barrier in the grain boundary region. Thus, the nonlinear current-voltage characteristics of ZnO-based varistors are fundamentally attributed to the nature of the grain boundary barrier layer between the relatively conductive ZnO grains [10-12].

Recently, it was revealed that zinc oxide having V_2O_5 as the only additive also exhibits non-ohmic behavior with a varistor property similar to that of ZnO-Bi_2O_3, ceramics. Moreover, there is an additional advantage for the ZnO-V_2O_5 system in that the ceramics can be sintered at relatively low temperature, i.e. about 900°C [l3]. The origin of their non-ohmic behavior lies in their microstructure, where ZnO grains are three-dimensionally separated from each other by grain boundary layers formed by the reactions of additives with each other and with ZnO [14]. The current voltage (I -V) characteristics are dependent on the detailed microstructure of ZnO ceramics [15]. It is generally accepted that the secondary phases are predominantly δ-Bi_2O_3, $Zn_7Sb_2O_{12}$ (spinel) and $Zn_2Bi_3Sb_3O_{14}$ (pyrochlore) although the role of individual additives and their reaction products in determining the nonlinear electrical properties is not fully understood [16-18]. In the ZnO-Bi_2O_3 system, antimony oxide is usually added so as to react with ZnO and Bi_2O_3 forming a liquid phase during the sintering process and playing an important role in improving the varistor characteristics [19]. Vanadium oxide doped ZnO system exhibits multifunctional properties, which makes it an interesting material for technological applications. Single phase ZnO-V_2O_5 system has been considered as a diluted magnetic semiconductor (DMS) material, as ferromagnetism in DMS is one of the interesting problems of this century in condensed matter physics [20]. Ferromagnetism in vanadium doped ZnO was predicted theoretically by Sato and Yoshida [21] and very few experimental researches on V: ZnO powders were reported [22].

ZnO-V_2O_5 system is interesting not only in terms of its room temperature ferromagnetism but also as a transparent ferromagnetic material [23]. On the other hand, multi-phase ZnO-V_2O_5 exhibits varistors behavior which is also quite interesting because in all metal oxide doped ZnO systems, varistor behavior appear due to greater metal ion but in ZnO-V_2O_5 smaller vanadium ion is responsible [24-28]. For proper understanding of different features of ZnO-V_2O_5 system like the formation of different phases, arise of ferromagnetic behavior, change in structure due to vanadium doping, optical band gap tuning, the appearance of vibrational modes induced by vanadium doping, etc. a detailed study is required to cover these aspects. Although magnetic properties of a vanadium doped ZnO system are recently of interest but structural, compositional and vibrational characterization of this material has rarely been reported. With $3d^3$ $4s^2$ electron configuration, Vanadium doping is expected to modify the defective structure and optical properties of ZnO.

MATERIALS AND METHODS

Reagent grade raw materials were used in compositions suggested, thus ZnO and V_2O_5 chemical grade oxides were used. Five mixes were suggested to study the effect of vanadium oxide alone in a binary system ZnO plus V_2O_5 are given in Table 1. Prepared ZnO was wet ground in a ball for a period of 3 hours to pass 200 mesh sieves. The slurry was dried overnight and used to fulfill the above-mentioned mixes. The mixes were weighed in the suggested proportions, wet milled to ensure through mixing of the different compositions then dried at 110°C.

Two discs were used, the first one has 1.2 cm diameter and 0.2 cm thickness and the second disc has 5 cm diameter and 0.2 cm thickness. These two discs were processed by a semi-dry press method under 70 KN. Small specimens were subjected to thermal treatment to select the proper maturing temperature for each mix. Three discs were always fired in muffle kiln with a rate of heating of 5 °C /min in the temperature range between 800 -1220° C and for 2 hours. The sinter- ability of the different samples was determined in terms of physical properties. The optimum firing temperature for each mix was deduced from the determination of the following parameters; firing shrinkage, apparent porosity, bulk density and water absorption. The method given is according to the ASTM standard (C71, C72) [29].

The phase purity of the samples is examined using X-ray diffract meter with Cu-Ka radiation. Microstructural characterization of the samples is performed with a scanning electron microscope) SEM). The DC electrical measurements at room temperature are performed with an electrometer (model 6517, Keithley), 5 kV DC power supply and digital multimeter. High-quality silver paint is used for electrical contacts. The PM 6304 programmable automatic RCL meter was used for precise measurements of resistance, capacitance and inductance. From the measured values of capacitance, the dielectric constant at all frequency from 1 to 20 kHz was calculated at constant temperature.

Table 1: The mixes chosen for the study

Mix oxides	V0	V1	V2	V3	V4	V5
ZnO(mol%)	100	99.9	99.7	99.5	99.3	99
V_2O_5(mol%)	-	0.1	0.3	0.5	0.7	1

RESULTS AND DISCUSSTION

Results of water absorption are shown in Table 2 and Figure 1. A decrease in water absorption was recorded with rise in maturing temperature. Minimum water absorption was displayed in specimens fired at 1220 °C for 2 hours. The content of pores both and open governs the degree of densification reached at maturity. Minimum water absorption in sample (V2) equal to 1.029 % which containing ZnO and 0.668 mol% V_2O_5, fired at 1220°C for 2 hours. Minimum water absorption was achieved at 1220°C for 2 hours and at sintering temperature above 1250 °C the water absorption of all samples increased. This increase has been attributed to the increased intergranular porosity resulting from discontinuous grain growth [30]. Results of firing shrinkage as a function of temperature of different mixes are given in Table 3 and also graphically plotted in Figure 2 showed an increase with rise in temperature. Maximum values of firing shrinkage were attained in specimens fired at 1220 °C for 2 hours. X-ray diffraction analysis of sintered sample reveals to the lattice constants of phase was change after sintering. Lattice constant of each sample were changed in different extents depending on the varistor composition. The XRD patterns of different mix namely V°, V1, V2, V3, V4 and V5 Present in Figure 3. It is evident that the main peaks present correspond to the contributing oxides namely ZnO and V_2O_5. Also, in these patterns, ZnO can be detected by the diffraction peak at about 2θ = 31.859 (d = 2.47°A), 2θ = 34.529 (d = 2.5954 °A), 2θ =36.343 (d = 2.47 °A), 2θ = 47.66 (d = 1.9056 °A), 2θ = 56.687 (d = 1.62253 °A), 2θ = 62.984 (d = 1.4746 °A), 2θ = 68.049 (d = 1.3766 °A), 2θ = 66.482 (d = 1.40525 °A), 2θ = 77.05 (d = 1.2367 °A).

The addition of V_2O_5 decreases the crystal size of ZnO and exerted no significant trend on the change of degree of crystal. There is a shift in the values of 2θ and as a result in the calculated values for lattice spacing of ZnO with addition of V_2O_5 maximum shift of (0.02-05 °A) was recorded in mix containing 0.3 Wt% V_2O_5. The $Zn_3(VO_4)_2$ is formed when ZnO- V_2O_5 system is sintered at high temperature and that acts as liquid phase sintering aid. The revealed phases are identical to those in the binary ZnO-V_2O_5 system. The SEM of standard V° present in Figure 4 shows ZnO grains of various size

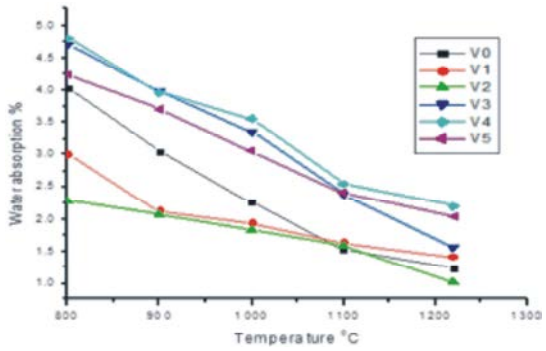

Fig. 1: Water absorption of different mixes

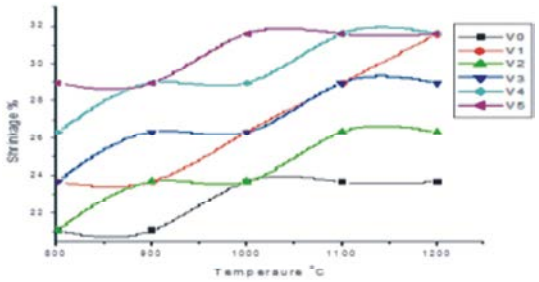

Fig. 2: Firing shrinkage % of different mixes

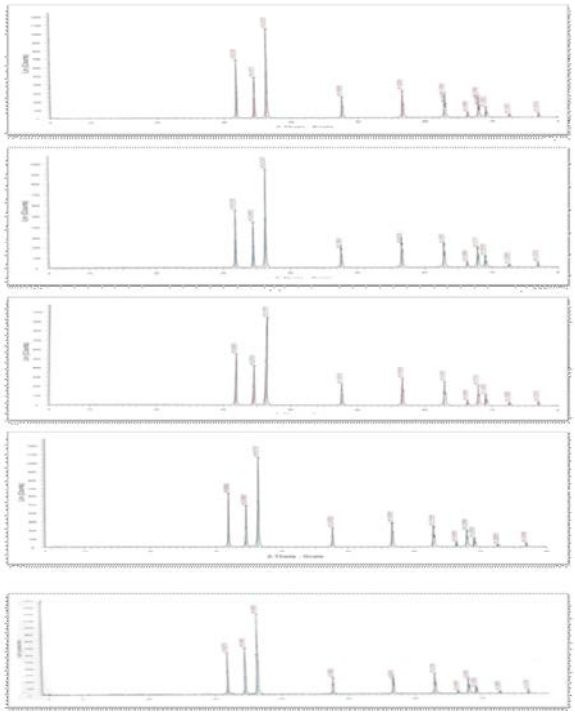

Fig. 3: XRD patterns of different mixes.

2 and 5 µm. Submicron process occur at triple points at grain corners, which ZnO-ZnO grain junctions are devoid of them, Figure 5. ZnO and V_2O_5, showed a homogeneous primary particle size of 2-5 µm, ZnO grains dissolution of

Table 2: Water absorption of different mixes

Temperature°C /Sample	800	900	1000	1100	1220
V0	4.033	3.044	2.261	1.5341	1.232
V1	3.0072	2.1231	1.9341	1.6291	1.423
V2	2.29	2.0729	1.8381	1.5931	1.029
V3	4.697	3.9804	3.352	2.393	1.5601
V4	4.803	3.964	3.556	2.556	2.197
V5	4.229	3.702	3.0522	2.4072	2.035

Table 3: Firing shrinkage of different mixes

Sample / Temperature °C	V_0	V_1	V_2	V_3	V_4	V_5
800	21.0526	23.6842	21.0526	23.6842	26.3158	28.9473
900	21.0526	23.6842	23.6842	26.3158	28.9473	28.9473
1000	23.6842	26.3158	23.6842	26.3158	28.9473	31.5789
1100	23.6842	28.9473	26.3158	28.9473	31.5789	31.5789
1220	23.6842	28.9473	26.3158	28.9473	31.5789	31.5789

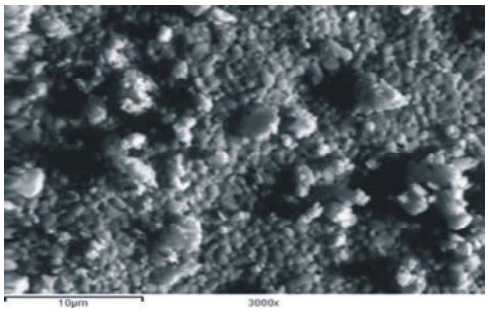

Fig. 4: SEM of mix V_0, thermally etched surface X=3000

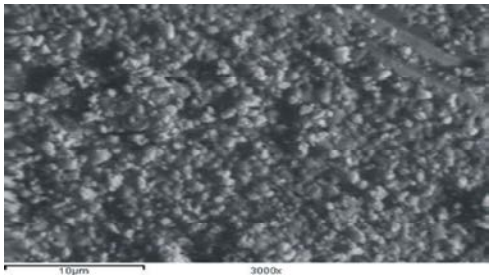

Fig. 5: SEM of V_1, thermally etched, fired at 1000 °C showed two phase grains agglomerates of various size X=3000.

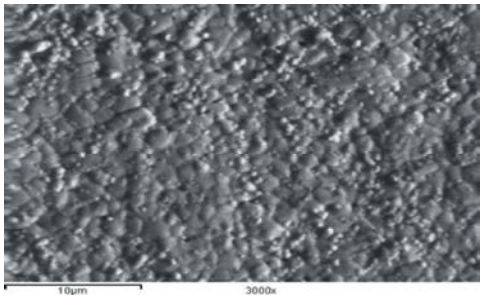

Fig. 6: SEM of V2, thermally etched showed two phase ZnO grain and intergranular phase X=3000

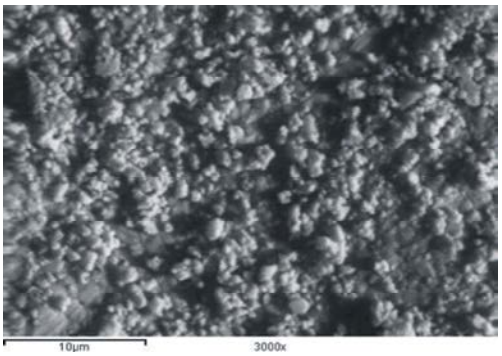

Fig. 7: SEM of V3, thermally etched, general view X=3000

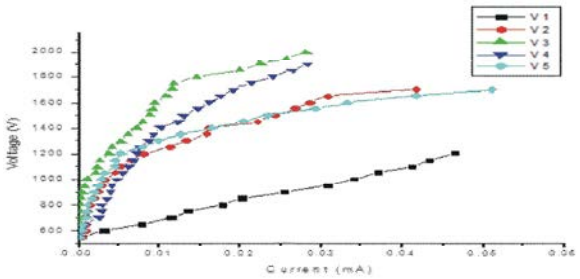

Fig. 8. I-V Characteristics of different mixes.

V_2O_5 between ZnO grains as shown in Figures 6 & 7. The binary system (ZnO-V_2O_5) showed exaggerated ZnO grain growth, which previously studies have also reported [31-33]. The microstructural observations are consistent with the reported liquid-phase sintering mechanism for ZnO varistors containing V_2O_5 [31, 32,]. ZnO has an eutectic reaction with $Zn_3(VO_4)_2$ at ~890°C [30] and for sintering at > 900 °C it has been suggested that liquid phase of $Zn_3(VO_4)_2$ will enhance densification by solution and re-precipitation of ZnO. In all our specimens, the microstructure consisted of ZnO grain surrounded by a V-rich phase of $Zn_3(VO_4)_2$ indicative of liquid-phase sintering $Zn_3(VO_4)_2$ grains are usually embedded in ZnO grain or occurring at triple and multiple grain junctions and the observation is consistent with previous studies [32, 33]. A liquid phase sintering process might occur when the sintering temperature was higher than eutectic temperature, leading to the densification of the sintered body and the ZnO grains growth. Consequently, the samples were all composed of compact ZnO grains and the average grain size of ZnO -V_2O_5 increased up to 5µm.

The (I-V) characteristics were measured between 0 - 5 KV and current between 0 -10 mA. The effect of V_2O_5 is demonstrated in different mixes in Figure 8. All mixes exhibit non-ohomic relation. The curves show the conduction characteristics divide into two regions: an

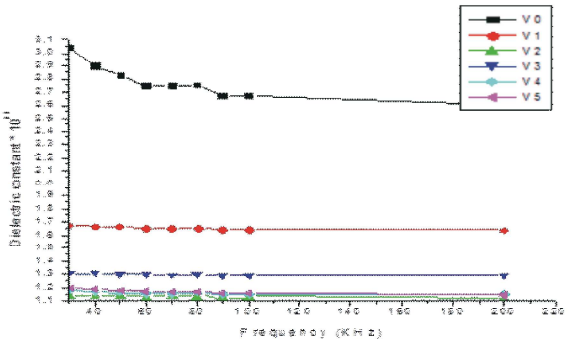

Fig. 9: AC Dielectric constant as function frequency at room temperature of different mixes.

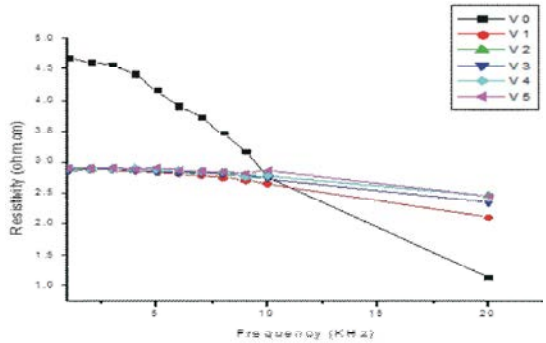

Fig. 10: Resistivity as a function of frequency for different mixes.

ohmic region before breakdown and a non-ohmic region after breakdown. The sharper the knee of the curves between the two regions, the better the nonohmic properties. In the binary system, samples V0, V1, V3, as shown in Figure 9, increasing the concentration of V_2O_5 leads to a gradual decrease of capacitance and consequently in dielectric constant as a function of frequency.

Low and high additions of mol % V_2O_5 showed more or less a constant dielectric value in the range of experimental frequency. The results of resistivity as a function of frequency of different, namely V0, V1, V2, V3, V4 and V5, containing ZnO and 0.223, 0.668, 1.11, 1.55 and 2.207 mol% V_2O_5, respectively are also graphically represented as a function of frequency in Fig. 10. The results show that the resistivity decreases with increasing frequency for all specimens. It can be deduced that the addition of V_2O_5 alone render ZnO conducting. Mix V0 showed a resistivity of 1.1192 at 20 kHz while other mixes, the values are ranged between 2.09 to 2.447. The relation between conductivity and frequency for different mixes of different groups increased with increasing frequency at room temperature. This may be attributed to the increase in the number of dipoles. The increase of frequency raised the conductivity because it increases ionic response to the field again this is related to intergranular material at the field again this is related to intergranular material at any particular temperature. This effect is associated to polarization currents arising from trapping states of various kinds and densities. The increase in frequency raised the conductivity as a result of the increase in ionic response to the field again this is related to inter-granular material. Pure ZnO is an insulating semiconductor while sintered ZnO is reasonably conducting. This conductivity probably drives from shallow donor levels in the ZnO associated with oxygen vacancies created in the ~ 1200 °C sintering process.

CONCLUSION

Minimum water absorption was displayed in specimens fired at 1200 °C for 2 hours. The content of pores both and open governs the degree of densification reached at maturity. Minimum water absorption does not mean maximum densification. Also the content of closed pores affect to a greater extent the sinter ability of the varistor body produced. The (I-V) characteristics of different mixes show clearly non-linear behavior. The characteristic curves of different groups are greatly divided into two regions, that is pre breakdown at low voltage region and an off-state and non-linear properties as an on-state high voltage region, the sharper the knee of the curves between the two regions, the better the non-linearity. In the binary system, the increase of concentration of V_2O_5 leads to a gradual decrease of capacitance and consequently in dielectric constant as a function of frequency. Low and high additions of mol % V_2O_5 showed more or less a constant dielectric value in the range of experimental frequency. The addition of V_2O_5 alone render ZnO conducting. The SEM of standard ZnO shows ZnO grains of various size 2 and 5 µm. Submicron pores occur at triple points at grain corners, which ZnO-ZnO grain junctions are devoid of them. The binary system (ZnO-V_2O_5) showed exaggerated ZnO grain growth. A liquid phase sintering process might occur when the sintering temperature was higher than eutectic temperature, leading to the densification of the sintered body and the ZnO grains growth.

ACKNOWLEDGEMENTS

The authors are grateful to Omar Al-Mukhtar University, Al-Bayda, Libya for financial support.

REFERENCES

1. Trontelj, M. and D. Kojar, 1978. J. Mater. Sci., 13: 1832.
2. Marshall, Jr. P.A., D.P. Enright and W.A. Weyl, 1952. Proceedings of the International Symposium on the Reactivity of Solids, Gothenburg, pp: 273.
3. Chu, M., M.N. Rahaman and L.C. 1991. J.Am. Ceram. Soc., 74(6): 1217.
4. Huckabee, M.L. and H. Palmour, 1972. American Ceramic Society Bulletin, 51(7): 574.
5. Lou, L.F., 1979. J. Appl. Phys., 50: 555.
6. Morris, W.G., 1973. J. Am. Ceram. Sot., 56: 360.
7. Wong, J., 1980. J. Appl. Phys., 51: 4453.
8. Levinson, L.M., H.R. Philipp and G.D. Mahan, 1989. in: Ceramic transaction, Vol. 3, ed. L.M. Levinson (American Ceramic Society, Weterville, OH, 145.
9. Bhushan, B., S.C. Kashyap and K.L. Chopra, 1981. Appl. Phys. Letters, 38: 160 .
10. Levine, J.D. and C.R.C. Crit, 1975. Rev. Solid State Sci., 5: 597.
11. Mahan, G.D., L.M. Levinson and H.R. Philipp, 1979. J. Appl. Phys., 50: 2799
12. Pike, G.E., 1982. Mater. Res. Sot., 5: 369.
13. Tsai, J.K. and T.B. Wu, 1994. J. Appl. Phys., 76: 4817.
14. Tnada, M., 1978. J. AppL Phys., 7: 1.
15. Olsson, E., G. Dunlop and R. Osterlund, 1993. J. Am. Ceram. Soc., 76: 65.
16. Inada, M., 1980. J. Appl. Phys., 19: 409.
17. Wong, J. and W.G. Morris, 1974. Bull Am. Ceram. Soc., 53: 816.
18. Salmon, R., M. Glaciet, G. Leflem and P. Hagenmuller, 1980. J. Solid State Chem., 34: 377.
19. Takemura, T., M. Kobayashi, Y. Takada and K. Sato, 1987. Am. Ceram. Soc., 70: 237
20. Koleva, M.E., P.A. Atanasov, N.N. Nedialkov, H. Fukuoka and M. Obara, 2007. Appl. Surf. Sci., 254: 1228.
21. Sato, K. and H.K. Yoshida, 2000. J. Appl. Phys., 39: 555.
22. Maensiri, S., C. Masingboon, V. Promarak and S. Seraphin, 2007. Opt. Mater., 29: 1700.
23. Saeki, H., H. Tabata and T. Kawai, 2001. Solid State Commun., 120: 439
24. Hng, H.H. and L. Halim, 2003. Mater. Lett., 57: 1411.
25. Tsai, J.K. and T.B. Wu, 1996. Mater. Lett., 26: 199.
26. Hng, H.H. and K.M. 1999. Knowles, J. Eur. Ceram. Soc., 19: 721.
27. Hng, H.H. and K.M. Knowles, 2000. J. Am. Ceram. Soc., 83: 2455.
28. Alnual book of ASTM standards, 1966. ASTM standards on ceramics, American society for testing and material.
29. Armstrong, T.R., L.E. Morgens, A.K. Maurice and R.C. Buchanan, 1989. J. Am. Ceram. Soc., 72: 605.
30. Tsai, J.K. and T.B. Wu, 1995. Appl. Phys. Part 1, 34: 6452.
31. Chen, C.S., C.T. Kuo, T.B. Wu, I.N. Lin, 1997. J. Appl. Phys., Part 1, 36: 1169.
32. Kuo, C.T., C.S. Chen, I.N. Lin, 1998. J. Am. Ceram. Soc., 81: 2942.
33. Huiming, J.I., L.I. Cuixia, M. Hui, C. Guyou and Y. Jikang. 2005. J. Rare Earths, 23:214.+